Fast Water Waves in Stationary Surface Disk Arrays

Xinyu Zhao,[1] Xinhua Hu,[1,2,*] and Jian Zi[3]
[1]Department of Materials Science and Key Laboratory of Micro- and Nano-Photonic Structures (Ministry of Education), Fudan University, Shanghai 200433, China
[2]Peng Cheng Lab, Shenzhen 518000, China
[3]Department of Physics and Key Laboratory of Surface Physics, Fudan University, Shanghai 200433, China

(Received 14 June 2021; accepted 18 November 2021; published 15 December 2021)

Traditionally, the phase and group velocities of water waves can be increased by increasing water depth but possess upper bounds, which are related to the gravitational acceleration and difficult to exceed. Here, we theoretically propose and experimentally demonstrate that when water is covered with a periodic array of stationary rigid disks, both the gravitational acceleration and reduced water depth can be effectively increased in the lowest frequency band. As a result, fast water waves can occur in the system, with both the phase and group velocities exceeding those in water without disks. Unusual effects, such as total reflection at oblique incidence and unidirectional transmission of water waves, are further realized.

DOI: 10.1103/PhysRevLett.127.254501

Water waves are mechanical waves propagating along the surface of water, and the restoring force is provided by gravity [1,2]. Understanding and controlling of the propagation of water waves are of great significance in both hydrodynamics and ocean engineering [1,2]. A fundamental property of water waves is the dispersion $\omega(k_0)$, from which the phase velocity $v_{0,p} \equiv \omega/k_0$ and group velocity $v_{0,g} \equiv \partial\omega/\partial k_0$ can be derived, where ω is the angular frequency, $k_0 \equiv 2\pi/\lambda_0$ is the wave number, and λ_0 is the wavelength. For a fixed angular frequency ω, the phase and group velocities of linear water waves can be increased with increasing the water depth h_0, but possess upper bounds

$$v_{0,p} < g_0/\omega, \qquad v_{0,g} < \alpha g_0/\omega, \tag{1}$$

where $\alpha = 0.5998$ and g_0 is the gravitational acceleration [see Fig. 1(a)]. Such upper bounds of velocities, first established by Airy in 1841 [3], are valid for various frequencies and difficult to exceed.

Recently, the interaction of water waves with periodic structures, such as rippled bottoms, vertical cylinder arrays, and resonator arrays, has received much attention [4–24]. In such periodic systems, the dispersion of water waves is modified as $\omega(k_e)$ with k_e being the Bloch wave number, which is also called band structures [6–15]. Since k_e is restricted to the reduced Brillouin zone, the phase velocity, given by $v_{e,p} \equiv \omega/k_e$, can exceed that $(v_{0,p})$ in water without structures in high frequency bands. However, for the lowest frequency band, the phase velocity remains lower than that in water without structures. In addition, the group velocity, given by $v_{e,g} \equiv \partial\omega/\partial k_e$, cannot exceed that $(v_{0,g})$ in water without structures for all the frequency bands [16–24]. As a result, long water waves are usually slowed down when periodic structures are introduced in water.

In this Letter, we theoretically propose and experimentally demonstrate that when water is covered with a periodic array of stationary rigid disks, both the gravitational acceleration and reduced water depth can be effectively increased ($g_e > g_0$, $u_e > u_0$) in the lowest frequency band. As a result, both the phase and group velocities of long water waves can exceed those in water without disks [see Fig. 1(b)]. Unusual effects, such as total reflection at oblique incidence and unidirectional transmission, are further realized in water waves.

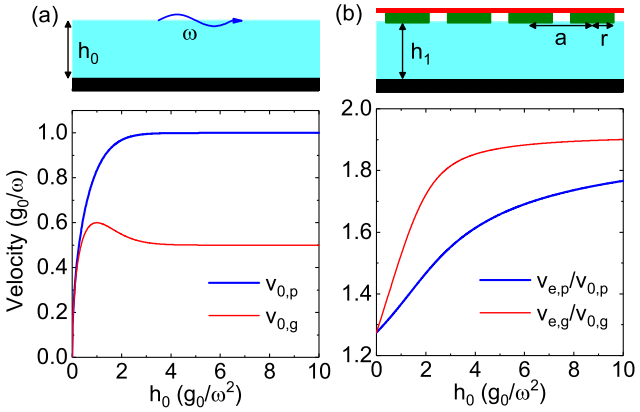

FIG. 1. Phase and group velocities of water waves with angular frequency ω. (a) Phase velocity $v_{0,p}$ and group velocity $v_{0,g}$ of water waves as functions of water depth h_0 in water without structures. (b) Ratios of $v_{e,p}/v_{0,p}$ and $v_{e,g}/v_{0,g}$ as functions of h_0, with $v_{e,p}$ and $v_{e,g}$ being the phase and group velocities of water waves in water covered with a square lattice of stationary rigid disks. The radius of disk $r = 0.35a$, the period of the array $a \ll g_0/\omega^2$, and the water depth under the disks $h_1 \approx h_0$.

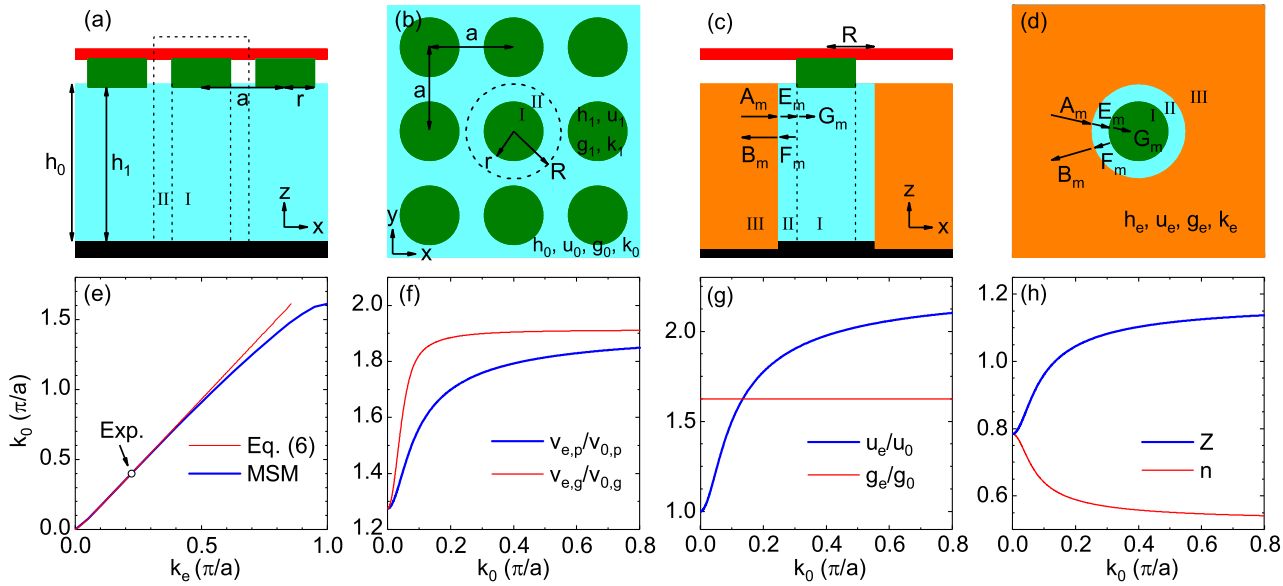

FIG. 2. Propagation of water waves in water covered with a square lattice of stationary rigid disks. The period of array is a. (a) and (b) Side and vertical views of the periodic system. (c) and (d) Side and vertical views of a water column which is covered with a stationary rigid disk and surrounded by an effective liquid. (e) Dispersion of water waves in the periodic system, where k_0 is the wave number in water without disks, the Bloch wave vector $\mathbf{Q}$ is in the x direction, and $k_e = |\mathbf{Q}|$. (f) Ratios of $v_{e,p}/v_{0,p}$ and $v_{e,g}/v_{0,g}$ as functions of k_0. (g) Ratios of g_e/g_0 and u_e/u_0 and (h) refractive index n and impedance Z of the periodic system as functions of k_0. The red rigid board above the disks are not shown in (b) and (d). In (e)–(h), the radius of disk $r = 0.35a$ and the water depth $h_1 \approx h_0 = 10a$.

We consider linear, inviscid, and irrotational water waves in water covered with a square lattice of circular rigid disks, which are mounted below a stationary rigid board, as shown in Figs. 2(a) and 2(b). The disks have a radius r, period a, filling ratio $f_s = \pi r^2/a^2$, and thickness larger than the amplitude of water waves. The water regions with a free surface and under the disks have a depth h_0 and h_1, respectively, where $h_1 < h_0$. Set $\mathbf{r} = (x, y)$ in the horizontal plane and z as the vertical axis.

For harmonic water waves, a velocity potential $\Phi_j(\mathbf{r}, z)e^{-i\omega t}$ can be introduced, so that $\nabla\Phi_j$ and $\partial\Phi_j/\partial z$ are the velocity of water particle in the horizontal and vertical directions with $\nabla \equiv (\partial/\partial x, \partial/\partial y)$, where $j = 0$ and 1 for the water regions with a free surface and under the disks, respectively. Φ_j satisfies the three-dimensional Laplace's equation [1,2]

$$\nabla^2\Phi_j + \frac{\partial^2\Phi_j}{\partial^2 z} = 0, \tag{2}$$

subjected to the boundary condition of $\partial\Phi_j/\partial z = 0$ at the bottom ($z = 0$). $\partial\Phi_0/\partial z = (\omega^2/g_0)\Phi_0$ at the air-water interface ($z = h_0$), while $\partial\Phi_1/\partial z = 0$ at the disk-water interface ($z = h_1$) which can also be written as $\partial\Phi_1/\partial z = (\omega^2/g_1)\Phi_1$ with $g_1 = \infty$. Therefore, we have $\Phi_j(\mathbf{r}, z) = \varphi_j(\mathbf{r})\cosh(k_j z)/\cosh(k_j h_j)$ with φ_j satisfying the two-dimensional Helmholtz equation

$$\nabla^2\varphi_j + k_j^2\varphi_j = 0. \tag{3}$$

The wave number k_j can be obtained from the dispersion

$$\omega = \sqrt{g_j u_j} k_j \tag{4}$$

with the reduced water depth

$$u_j = [\tanh(k_j h_j)]/k_j. \tag{5}$$

Since a stationary solution is sought, the frequency ω is the same in all the regions. The dispersion can also be written as $\omega^2 = g_j k_j \tanh(k_j h_j)$. For a given angular frequency ω, two real numbers of k_j and many imaginary ones can be obtained from the dispersion, corresponding to propagating and evanescent waves, respectively. In the following, we will only consider the propagating waves, so that the flow can be expressed as $\mathbf{S}_j \equiv \int_0^{h_j}(\nabla\Phi_j)dz = u_j\nabla\varphi_j$. At the interface between different water regions, both the potential φ_j and flow $u_j\nabla\varphi_j$ should be continuous. Although the evanescent waves are neglected, the results remain high accuracy for $k_0 < 0.5\pi/a$ [25].

We note that the vertical vibration of the upper surface of water $\eta_j(\mathbf{r}, t) = \mathrm{Re}[i\varphi_j(\mathbf{r})e^{-i\omega t}\omega/g_j]$. For water under disks, $k_1 = 0$ and $u_1 = h_1$. For water with a free surface, $u_0 \approx h_0$ for $h_0 \ll g_0/\omega^2$ but $u_0 < g_0/\omega^2$, giving rise to the upper bounds of velocities in Eq. (1).

We then derive analytic formulas for the effective parameters (g_e, u_e) of the periodic system with the coherent-potential-approximation method [16,18,26]. We consider a circular water column with radius $R = a/\sqrt{\pi}$

(so that $\pi R^2 = a^2$) and height h_1, which is covered with a stationary rigid disk of radius r and surrounded by an effective liquid with parameters (g_e, u_e, h_e, k_e), as shown in Figs. 2(c) and 2(d). The liquid waves in the effective liquid can also be described by Eqs. (2)–(5) but with $j = e$, where the dispersion is given by

$$\omega = \sqrt{g_e u_e} k_e \tag{6}$$

with $u_e = [\tanh(k_e h_e)]/k_e$. By using the cylindrical coordination (ρ, θ) with the origin at the center of the disk, we have $\varphi_1 = \sum_m G_m J_m(k_1\rho)e^{im\theta}$ for region I ($\rho \le r$), $\varphi_0 = \sum_m [E_m J_m(k_0\rho) + F_m H_m(k_0\rho)]e^{im\theta}$ for region II ($r \le \rho \le R$), and $\varphi_e = \sum_m [A_m J_m(k_e\rho) + B_m H_m(k_e\rho)]e^{im\theta}$ for region III ($\rho \ge R$). Here, the Bessel (Hankel) function J_m (H_m) represents the mth cylindrical incident (scattering) wave. At the interfaces between different water regions, both the potential φ_j and flow $u_j \nabla \varphi_j$ should be continuous [$\varphi_1(r) = \varphi_0(r)$, $\varphi_0(R) = \varphi_e(R)$, $u_1[\partial\varphi_1(r)/\partial\rho] = u_0[\partial\varphi_0(r)/\partial\rho]$, and $u_0[\partial\varphi_0(R)/\partial\rho] = u_e[\partial\varphi_e(R)/\partial\rho]$]. It can thus be shown that scattering waves cannot be generated in the effective medium ($B_m = 0$ which defines the effective medium) when

$$-\frac{u_0 k_0 J_m'(k_0 R) - J_m(k_0 R) T_{e,m}}{u_0 k_0 H_m'(k_0 R) - H_m(k_0 R) T_{e,m}} = -\frac{u_0 k_0 J_m'(k_0 r) - J_m(k_0 r) T_{1,m}}{u_0 k_0 H_m'(k_0 r) - H_m(k_0 r) T_{1,m}} \tag{7}$$

where $T_{e,m} = u_e k_e J_m'(k_e R)/J_m(k_e R)$, $T_{1,m} = u_1 k_1 J_m'(k_1 r)/J_m(k_1 r)$, and the second term is the mth order scattering coefficient ($D_m \equiv F_m/E_m$) of the water column under the disk. When $k_0 a$, $k_e a \ll 1$ [25], Eq. (7) with the two lowest orders ($m = 0$ and 1) becomes

$$g_e = g_0/(1 - f_s), \qquad u_e = u_0(1 + p)/(1 - p), \tag{8}$$

where $p = f_s(u_1 - u_0)/(u_1 + u_0)$. For stationary surface disk arrays ($u_1 = h_1 \approx h_0$), we have $u_0 < u_e < u_0(1 + f_s)/(1 - f_s)$. For bottom-mounted rigid cylinder arrays ($u_1 = h_1 = 0$), we have $g_e = g_0/(1 - f_s)$ and $u_e = u_0(1 - f_s)/(1 + f_s)$, consistent with our previous derivations [16].

The ratios of the phase and group velocities in the disk array to those without disks can be expressed as

$$\frac{v_{e,p}}{v_{0,p}} = \frac{k_0}{k_e}, \qquad \frac{v_{e,g}}{v_{0,g}} = \frac{\partial k_0}{\partial k_e}. \tag{9}$$

Since $k_e = n k_0$ and the refractive index $n = \sqrt{g_0 u_0/(g_e u_e)}$, we have $v_{e,p}/v_{0,p} = 1/n$ and $v_{e,g}/v_{0,g} = 1/[n + k_0(\partial n/\partial k_0)]$. When $\partial n/\partial k_0 = 0$, $v_{e,p}/v_{0,p} = v_{e,g}/v_{0,g}$. But if $\partial n/\partial k_0 \neq 0$, the two ratios of velocities can be completely different. Therefore, for water waves in water pierced with a bottom-mounted split-tube array, $v_{e,p} \gg v_{0,p}$ but $v_{e,g} \approx 0$ above the resonant band gap [25].

The ratios of velocities can be calculated with using Eq. (8), as shown in Fig. 1(b). For a fixed angular frequency ω, the phase and group velocities of long water waves in the stationary rigid disk array increase with increasing the water depth, but possess upper bounds

$$v_{e,p} < \beta g_0/\omega, \qquad v_{e,g} < \gamma g_0/\omega. \tag{10}$$

Since $\beta = \sqrt{1 + f_s}/(1 - f_s)$, $\gamma > \alpha$, and $\gamma = \beta/2$ for $f_s > 0.37$, such upper bounds can exceed those in Eq. (1) for water with a free surface.

To check the accuracy of the analytic formulas above, we use the multiple scattering method (MSM), which includes high order cylindrical waves, to numerically calculate the dispersion of water waves in the periodic disk array [11,12,16]. Figure 2(e) shows the dispersion $k_0(k_e)$ of Bloch water waves in water covered with a stationary rigid disk array, where $r = 0.35a$, $h_1 \approx h_0 = 10a$, $k_e = |\mathbf{Q}|$, and the Bloch wave vector $\mathbf{Q}$ is in the x direction. The value of k_0 is independent of the direction of $\mathbf{Q}$ for $k_0 < 1.4\pi/a$. The dispersion of water waves in the system is also obtained by Eqs. (6) and (8), as shown as the red line in Fig. 2(e). Excellent agreement can be seen between the numerical and analytical results, especially in low frequencies ($k_0 < \pi/a$). Figure 2(f) shows the ratios of $v_{e,p}/v_{0,p}$ and $v_{e,g}/v_{0,g}$ in the disk array. The velocity ratios are 1.28 at zero frequency, and they can increase with increasing frequency and be about 1.9 in high frequencies.

Figure 2(g) shows the effective parameters (g_e, u_e) for the above system. We can see that in the lowest frequency band, $g_e = 1.63 g_0$ and u_e/u_0 increases from 1 to 2.17 with increasing the frequency. Hence, both the phase and group velocities of long water waves in the disk array can exceed those in water without disks. Using the g_e and u_e, the refractive index n and impedance $Z = \sqrt{u_e g_0/(g_e u_0)}$ can also be obtained for the system [Fig. 2(h)]. As the frequency increases, the impedance Z increases from 0.78 to 1.16, while the refractive index n decreases from 0.78 to 0.53.

When a plane water wave propagates from water with a free surface to that covered with a stationary rigid disk array, reflection and refraction of waves will occur at the surface of the disk array. The corresponding amplitude reflection coefficient $r_A = (\cos\theta_i - Z\cos\theta_r)/(\cos\theta_i + Z\cos\theta_r)$, where θ_i and θ_r are the incident and refraction angles following the Snell law of $\sin\theta_i = n \sin\theta_r$. Since $0 < n < 1$, total reflection of water waves can occur for incident angles above a critical angle $\theta_c = \arcsin(n)$.

To verify the above prediction, we perform multiple-scattering simulations, which solve the stationary problems for impinging a plane water wave upon a ten-layer array of surface disks on the water, with parameters of $k_0 = 0.4\pi/a$,

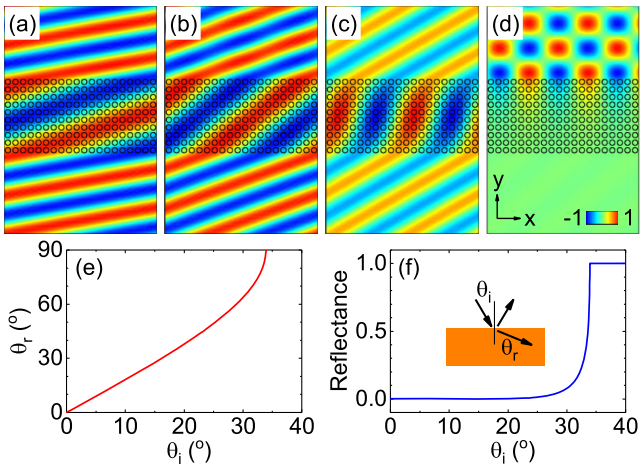

FIG. 3. Impinging of a plane water wave upon a water region covered with a ten-layer array of stationary rigid disks. The parameters are $r = 0.35a$, $h_1 \approx h_0 = 10a$, and $k_0 = 0.4\pi/a$. The disk array extends to infinity in the x direction. (a)–(d) Simulated patterns of $\mathrm{Re}(\varphi)$ in the x-y plane at different incident angles $\theta_i = 10°, 20°, 30°, 40°$. (e) Refraction angle θ_r and (f) reflectance at the surface of the disk array as a function of incident angle θ_i.

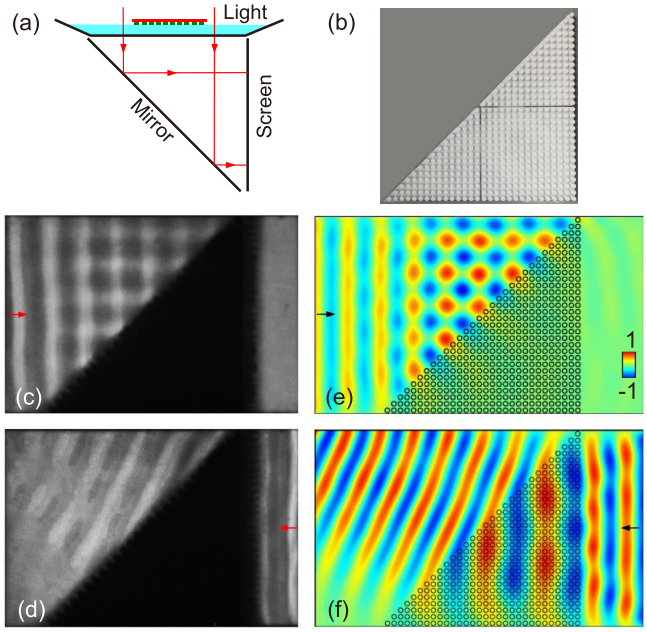

FIG. 4. Unidirectional transmission of water waves through water covered with a stationary rigid disk array with an isosceles right triangle shape. The parameters are $h_0 = 10$ cm, $h_1 = 9.9$ cm, $r = 3.5$ mm, $a = 10$ mm, and $\lambda_0 = 50$ mm. (a) Schematic diagram of the experimental setup. Water is placed in a vessel with a transparent bottom and slanted sides. Using a mirror and collimated light, the pattern of water waves can be projected onto a screen. (b) Photograph of the disk array which consists of 465 PLA disks mounted on a rigid board. (c) and (d) Photographs of wave patterns. (e) and (f) Simulated patterns of $\mathrm{Re}(\varphi)$ in the x-y plane. Water waves are incident from the left of the array in (c) and (e), while they are from the right in (d) and (f).

$r = 0.35a$, and $h_1 \approx h_0 = 10a$. For incident angles $\theta_i = 10°$, 20°, 30°, transmitted waves occur in the disk array, with refraction angles $\theta_r = 18°, 38°, 64°$ [Figs. 3(a)–3(c)]. Water waves can be totally reflected at $\theta_i = 40°$, resulting in interference pattern above the disk array [Fig. 3(d)]. Such simulated patterns agree well with analytic results shown in Figs. 3(e) and 3(f). Here, the disk array has a refractive index $n = 0.56$ and critical angle $\theta_c = 33.9°$. Since the impedance is close to unity ($Z = 1.10$), the reflection at the surface of the disk array is less than 8% for $\theta_i < 30°$, benefiting the construction of transmission-type devices for water waves.

Based on the above results, more fascinating effects, such as unidirectional water-wave transmission, can be proposed and experimentally verified, as shown in Fig. 4. Here, we adopted a vessel with a transparent bottom and slanted sides, so that reflected waves will not be generated at the boundaries. Water is placed in the vessel and then covered with a stationary rigid disk array with an isosceles right triangle shape, where the depth $h_0 = 10$ cm and $h_1 = 9.9$ cm [Fig. 4(a)]. The array consists of 465 rigid disks with $r = 3.5$ mm, $a = 10$ mm, and height of 8 mm, which is mounted on a rigid board and fabricated with polylactic acid (PLA) by means of 3D-printing technology [Fig. 4(b)]. A Gaussian water-wave beam with width of 28 cm and wavelength $\lambda_0 = 50$ mm serves as the wave source. By using a projection apparatus [12,14,17,22], the wave patterns are visualized on a screen [Fig. 4(a)]. When water wave is incident on the hypotenuse of the disk array from the left, the incident angle is larger than the critical angle. As a result, total reflection occurs, leading to interference pattern above the disk array [Fig. 4(c)]. However, as the water wave is impinged on the array from the right, transmission can occur. The outgoing wave is refracted at the hypotenuse of the array and not along the original direction [Fig. 4(d)]. Figures. 4(e) and 4(f) show the simulated wave patterns based on the multiple-scattering method. The simulated refraction angle in Fig. 4(f) is 25°, agreeing well with the experimental value of 24° in Fig. 4(d).

Fast water waves are reminiscent of superluminal effects in electromagnetics. If g^{-1}, u^{-1}, and φ are changed to permeability μ, permittivity ε, and magnetic field H_z, Eqs. (3) and (4) combined with the continuities of φ_j and $u_j \nabla \varphi_j$ are also valid for transverse-electric waves in 2D metamaterials. However, since appropriate constituent materials are not available, superluminal effects cannot be realized in transparent metamaterials and they have usually been observed in gain materials [27,28].

In summary, we have demonstrated that long water waves propagate in water covered with a periodic array of stationary rigid disks as if it has larger magnitudes of the effective gravitational acceleration g_e and the effective depth u_e given by Eq. (8). Since $g_e > g_0$ and $u_e > u_0$ in

the lowest frequency band, fast water waves can occur in the system, with both the phase and group velocities exceeding those in water without structures. Consequently, unusual effects, such as total reflection at oblique incidence and unidirectional transmission, have been realized in water waves. We anticipate that more effects and devices of water waves can be proposed and realized in water covered with stationary rigid disk arrays, and they could find applications in coastal protection and ocean wave energy extraction [29,30].

This work was supported by the National Key Research and Development Program of China (2018YFA0306201) and NSFC (61422504 and 11574037).

*huxh@fudan.edu.cn

[1] H. Lamb, *Hydrodynamics* (Cambridge University Press, Cambridge, England, 1995).
[2] C. C. Mei, *The Applied Dynamics of Ocean Surface Waves* (World Scientific, Singapore, 1989).
[3] G. B. Airy, in *Encyclopaedia Metropolitana*, edited by H. J. Rose *et al.* (Taylor, London, 1841).
[4] A. D. Heathershaw, Nature (London) **296**, 343 (1982); C. C. Mei, J. Fluid Mech. **152**, 315 (1985); J. T. Kirby, J. Fluid Mech. **162**, 171 (1986).
[5] M. W. Dingemans, *Water Wave Propagation over Uneven Bottoms* (World Scientific, Singapore, 1997); J. W. Miles, J. Fluid Mech. **28**, 755 (1967); Y. Tang, Y. Shen, J. Yang, X. Liu, J. Zi, and X. Hu, Phys. Rev. E **73**, 035302(R) (2006).
[6] M. Torres, J. P. Adrados, and F. R. Montero de Espinosa, Nature (London) **398**, 114 (1999); M. Torres, J. P. Adrados, F. R. Montero de Espinosa, D. Garcia-Pablos, and J. Fayos, Phys. Rev. E **63**, 011204 (2000).
[7] X. Hu, Y. Shen, X. Liu, R. Fu, and J. Zi, Phys. Rev. E **68**, 066308 (2003).
[8] Y. Shen, K. Chen, Y. Chen, X. Liu, and J. Zi, Phys. Rev. E **71**, 036301 (2005).
[9] S. Wu, Y. Wu, and J. Mei, New J. Phys. **20**, 023051 (2018); S. Wu and J. Mei, Europhys. Lett. **123**, 59001 (2018).
[10] P. McIver, J. Fluid Mech. **424**, 101 (2000); C. M. Linton and D. V. Evans, J. Fluid Mech. **215**, 549 (1990); H. Kagemoto and D. K. P. Yue, J. Fluid Mech. **166**, 189 (1986).
[11] X. Hu, Y. Shen, X. Liu, R. Fu, J. Zi, X. Jiang, and S. Feng, Phys. Rev. E **68**, 037301 (2003).
[12] X. Hu, Y. Shen, X. Liu, R. Fu, and J. Zi, Phys. Rev. E **69**, 030201(R) (2004).
[13] T. S. Jeong, J. E. Kim, and H. Y. Park, Appl. Phys. Lett. **85**, 1645 (2004); A. J. Archer, H. A. Wolgamot, J. Orszaghova, L. G. Bennetts, M. A. Peter, and R. V. Craster, Phys. Rev. Fluids **5**, 062801(R) (2020).
[14] N. Laforge, V. Laude, F. Chollet, A. Khelif, M. Kadic, Y. Guo, and R. Fleury, New J. Phys. **21**, 083031 (2019).
[15] Y. Meng, Y. Hao, S. Guenneau, S. Wang, and J. Li, New J. Phys. **23**, 073004 (2021).
[16] X. Hu and C. T. Chan, Phys. Rev. Lett. **95**, 154501 (2005).
[17] J. Yang, Y. F. Tang, C. F. Ouyang, X. H. Liu, X. Hu, and J. Zi, Appl. Phys. Lett. **95**, 094106 (2009); Z. Wang, P. Zhang, X. Nie, and Y. Zhang, Europhys. Lett. **108**, 24003 (2014).
[18] X. Hu, C. T. Chan, K. M. Ho, and J. Zi, Phys. Rev. Lett. **106**, 174501 (2011); X. Hu, J. Yang, J. Zi, C. T. Chan, and K. M. Ho, Sci. Rep. **3**, 1916 (2013).
[19] G. Dupont, F. Remy, O. Kimmoun, B. Molin, S. Guenneau, and S. Enoch, Phys. Rev. B **96**, 180302(R) (2017).
[20] L. G. Bennetts, M. A. Peter, and R. V. Craster, J. Fluid Mech. **854**, R4 (2018).
[21] C. Li, L. Xu, L. Zhu, S. Zou, Q. H. Liu, Z. Wang, and H. Chen, Phys. Rev. Lett. **121**, 104501 (2018).
[22] M. Farhat, S. Enoch, S. Guenneau, and A. B. Movchan, Phys. Rev. Lett. **101**, 134501 (2008).
[23] C. P. Berraquero, A. Maurel, P. Petitjeans, and V. Pagneux, Phys. Rev. E **88**, 051002(R) (2013).
[24] S. Zou, Y. Xu, R. Zatianina, C. Li, X. Liang, L. Zhu, Y. Zhang, G. Liu, Q. H. Liu, H. Chen, and Z. Wang, Phys. Rev. Lett. **123**, 074501 (2019).
[25] See Supplemental Material at http://link.aps.org/supplemental/10.1103/PhysRevLett.127.254501 for derivation of Eq. (8) and more results on the topic.
[26] P. Sheng, *Introduction to Wave Scattering, Localization, and Mesoscopic Phenomena* (Academic, New York, 1995).
[27] L. J. Wang, A. Kuzmich, and A. Dogariu, Nature (London) **406**, 277 (2000).
[28] R. Y. Chiao, Phys. Rev. A **48**, R34 (1993).
[29] K. Budal and J. Falnes, Nature (London) **256**, 478 (1975); J. Falnes, Applied Ocean Research **2**, 75 (1980); X. Garnaud and C. C. Mei, Proc. R. Soc. A **466**, 79 (2010).
[30] E. Callaway, Nature (London) **450**, 156 (2007); J. Cruz, *Ocean Wave Energy: Current Status and Future Perspectives* (Springer-Verlag, Berlin, 2008); X. L. Zhao, D. Z. Ning, Q. P. Zou, D. S. Qiao, and S. Q. Cai, Ocean Eng. **186**, 106126 (2019).